

Short communication

A Ni(II) ferromagnet with mixed pyridine-3,5-dicarboxylate-1,4-bis(imidazol-l-yl)butane heterobridges exhibiting long-range ordering and hysteresis loop

Min-Le Han ^{a,b}, Xue-Qian Wu ^a, Guo-Wang Xu ^a, Guo-Xuan Wen ^a, Dong-Sheng Li ^{a,*}, Lu-Fang Ma ^{b,*}^a College of Materials and Chemical Engineering, Hubei Provincial Collaborative Innovation Center for New Energy Microgrid, Key Laboratory of Inorganic Nonmetallic Crystalline and Energy Conversion Materials, China Three Gorges University, Yichang 443002, PR China^b College of Chemistry and Chemical Engineering, Henan Key Laboratory of Function-Oriented Porous Materials, Luoyang Normal University, Luoyang 471022, PR China

ARTICLE INFO

Article history:

Received 20 March 2016

Received in revised form 17 April 2016

Accepted 21 April 2016

Available online 22 April 2016

Keywords:

Ni^{II}-CPs

Pyridine-3,5-dicarboxylic acid

1,4-bis(imidazol-l-yl)butane

Magnetic property

ABSTRACT

A rare Ni-ferromagnet $[Ni(pdc)(bib)] \cdot 2H_2O$ (H_2pdc = pyridine-3,5-dicarboxylic acid, bib = 1,4-bis(imidazol-l-yl)butane) has been prepared, which possesses a 3D supramolecular network based on (3,5)-connected helical-armed 2D layers. Interestingly, at high temperature (>12.7 K), **1** exhibits a weak ferromagnetism, whereas at low temperature, it shows unusual long-range ordering (LRO) behaviors combining spin canting and hysteresis loop.

Crown Copyright © 2016 Published by Elsevier B.V. All rights reserved.

Coordination polymers (CPs) based on paramagnetic metal ions exhibiting extended structures are of intense current interest in the field of molecular magnetism and materials chemistry due to their various structural topologies and potential applications as functional materials [1–5]. These materials have also offered great opportunities to better understand fundamental magnetic phenomena, such as long-range ordering (LRO), spin canting, metamagnetism, anisotropy, relaxation dynamics, and so on [6]. As far as LRO is concerned, some complex and exotic behaviors have been revealed in molecular systems, for example, the combination of magnetic properties and other functions [7]. The key factors in the design and synthesis of these CPs with desirable properties and expected structures are mainly focused on the appropriate selection of nodes (metal ions or metal-including clusters) and spacers (organic ligands) [8]. When organic ligands coupled with a paramagnetic metal ion, these ligands may cite peculiar magnetic behaviors e.g. (anti)ferromagnetism, magnetoelectricity and multi-ferroicity [9]. Among organic ligands, multidentate ligands containing carboxylate and a pyridyl group, such as nicotinate, isonicotinate, and pyridine-dicarboxylate, have been frequently used in the preparation of magnetic materials, because the various coordination modes adopted

by the carboxylate group can transmit the magnetic coupling in different degrees, and the coordination of the pyridyl and carboxylate groups in these ligands may result in extended frameworks [10–14].

Meanwhile, the design, syntheses and applications of metal-organic hybrid materials based on mixed-ligands (multicarboxylate and flexible N-donor ligands) also have so far attracted unparalleled attention in research [15–17]. The flexibility of N-donor ligands can adopt different conformations and thus lead to distinct symmetries during the self-assembly process [18]. As part of our investigations on the structural diversity, magnetism properties of metal-organic hybrid materials based on mixed-ligands, herein, pyridine-3,5-dicarboxylic acid (H_2pdc) and 1,4-bis(imidazol-l-yl)butane (bib) were selected as a bridging ligand and reacted with Ni(II) ions, giving rise to a new metal-organic hybrid materials, namely $[Ni(pdc)(bib)] \cdot 2H_2O$ (**1**). Moreover, their magnetic properties were also investigated and discussed in detail.

Reaction of H_2pdc with bib and Ni(II) acetate at 140 °C for 3 days under hydrothermal conditions generates green crystalline product **1** [19]. The compositions were confirmed by elemental analysis and IR spectra, and powder X-ray diffraction. Single crystal X-ray diffraction study [20] reveals that complex **1** crystallizes in a monoclinic system with space group $P2_1/n$ and has a 3-D supramolecular framework work based on 2-D layers. All Ni sites are six-coordinated with a distorted octahedron geometry by three carboxylate-oxygen atoms (O1, O2 and O3#1, symmetry code: #1, $-x + 1, y, z$) from two pdc^{2-} , one nitrogen atom (N1#2, symmetry code: #2, $-x + 1/2, y + 1/2,$

* Corresponding authors at: College of Materials and Chemical Engineering, China Three Gorges University, Yichang 443002, PR China.

E-mail addresses: lidongsheng1@126.com (D.-S. Li), mazhuxp@126.com (L.-F. Ma).

$-z + 1/2$) from pdc^{2-} , and two *trans*-nitrogen atoms (N2 and N5#2) from two bib ligands with the angle of N2-Ni1-N5#2 of 175.7° (Fig. S1, Supporting Information). The pdc^{2-} ligand adopts a (κ^1 - κ^1)-(κ^1)- μ_3 -bridge linking three Ni(II) ions to form a 2D layer, moreover, the bib ligand with TGG conformation ($T = \text{trans}$, $G = \text{gauche}$) bridge Ni(II) ions to generate a 2_1 helical chain along [010] axis with the pitch of 12.5 \AA , which decorate the 2D layer at two sides in an outward fashion, resulting in a interesting helical-armed 2D network. Analysis of the network topology of **1** reveals that each Ni(II) center acts as a 5-connected node to connect three pdc^{2-} ligands and two bib spacers. And the pdc^{2-} ligands serve as the 3-connected nodes. Thus, a (3,5)-connected network with the point symbol of $(3\cdot 5^2)(3^2\cdot 5^3\cdot 6^4\cdot 7)$ is constituted (Fig. S2, Supporting Information[†]). There are evident intermolecular $\pi\cdots\pi$ stacking interactions between the adjacent imidazol ring of the adjacent 2D layers with co-facial distances of 3.66 and 3.78 \AA (Fig. 1), which extend these 2D with ABAB stacking fashions to build final 3-D supramolecular framework (Fig. 1).

Phase purities of the bulky materials of **1** were confirmed by powder X-ray diffraction (PXRD) patterns (see Fig. S3, SI[†]). The experimental and simulated PXRD patterns agree well with each other, confirming the good phase purity. Additionally, the thermogravimetric analysis of **1** was carried out under an air atmosphere (Fig. S4, Supporting Information[†]). The first weight lost of 7.8% was observed from $115\text{ }^\circ\text{C}$ to $198\text{ }^\circ\text{C}$ corresponding to the lost of free water molecules (calcd. 8.0%). Then pyrolysis of the sample occurred from 325 to $490\text{ }^\circ\text{C}$. The final residue of 24.2% is close to the calculated 24.6% based on NiO.

The temperature-dependent magnetic susceptibilities were measured on polycrystalline samples of **1** at 1000 Oe in the range of $1.8\text{--}300\text{ K}$ in Fig. 2. For **1**, the value of $\chi_M T$ at 300 K is $1.54\text{ cm mol}^{-1}\text{ K}$, which is larger than the spin-only value ($1.0\text{ cm mol}^{-1}\text{ K}$) expected for a magnetically isolated Ni(II) ion. The $\chi_M T$ value increases gradually upon cooling to ca. 35 K . Below this temperature, $\chi_M T$ value increases abruptly to a maximum of $4.69\text{ cm}^3\text{ mol}^{-1}\text{ K}$ at 12.7 K . Above 15 K , the temperature dependence of $1/\chi_M$ obeys the Curie-Weiss law with $C = 1.49\text{ cm K mol}^{-1}$ and $\theta = 4.91\text{ K}$, revealing dominant ferromagnetic

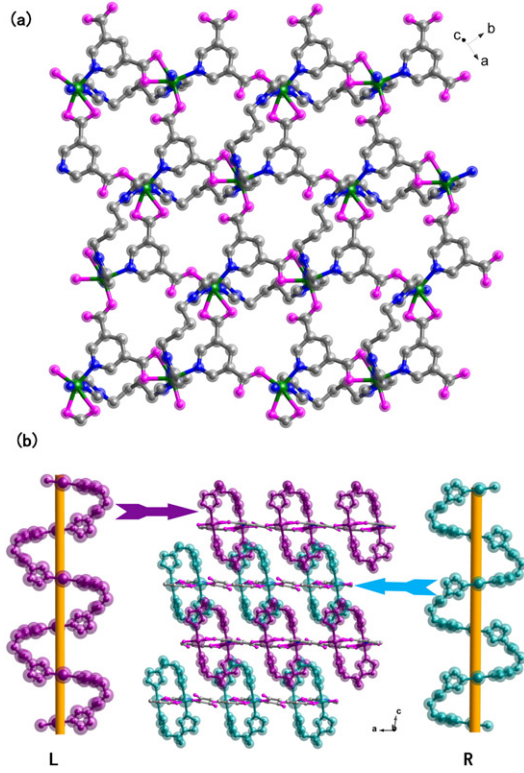


Fig. 1. (a) 2D layer in **1**. (b) 3D supramolecular structure of **1** and R- and L-handed helical chains.

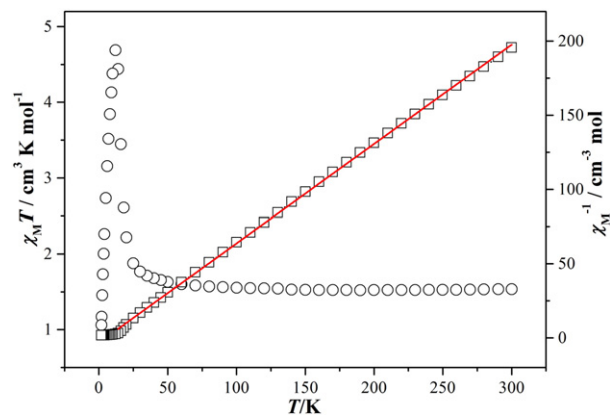


Fig. 2. Temperature dependence of $\chi_M T$ and $1/\chi_M$ for **1**. Open points are the experimental data, and the solid line represents the best fit obtained from the Curie-Weiss law.

interactions between the adjacent Ni(II) ions. Upon further cooling to 2 K , $\chi_M T$ decreases quickly. The steep declines in $\chi_M T$ at low temperature clearly indicate that a kind of spontaneous magnetization emerges. This phenomenon in a ferromagnetic system could be attributed to weak antiferromagnetism, owing to spin canting: the antiferromagnetic coupled spins from different sublattices are not parallel, but canted to each other, and the resulting net moments are correlated in a antiferromagnetic-like fashion and develop into LRO below the critical temperature.

To characterize the low-temperature behaviors of **1**, FC (field-cooled) and ZFC (zero-field-cooled) magnetization measurements were performed under 50 Oe (Fig. 3a). The ZFC magnetization shows

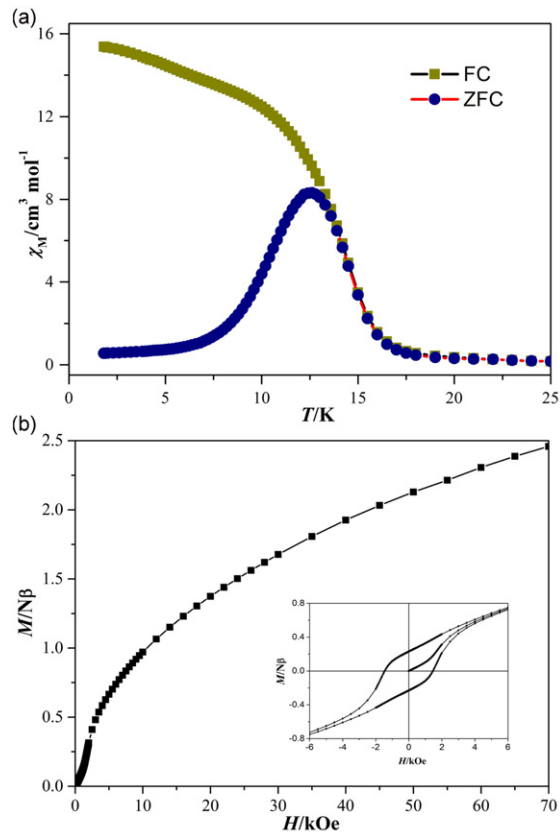


Fig. 3. (a) Low temperature dependence of the magnetic susceptibility (χ) for **1** measured under zero field cooling (ZFC) and field cooling (FC) conditions. (b) Field-dependent magnetization for **1** measured at 2.0 K . Insert: M versus H hysteresis loops for **1**.

a peak at 12 K and diverges from the FC magnetization at about 13 K. This kind of divergence further confirms a LRO of ferromagnetic interactions. In addition, the critical temperature (T_c), determined by the positions of the negative peak on the derivative dM/dT (M = magnetization) of FC data [7e], is 14.2 K. The T_c value is confirmed by the observation that the ZFC and FC curves merged at 50 Oe at 14.0 K. For **1**, the initial ZFC magnetization is very weak, increases very slowly upon warming up to 12.5 K, and then undergoes a rapid increase merge into FC curves at T_c .

The temperature dependences of the ac susceptibilities obtained under zero direct current (dc) field and 5 Oe ac field at frequencies 1, 10, 100, and 1000 Hz for **1** (Fig. S5, Supporting Information^{††}). Both in-phase (χ_M') and out-of-phase components (χ_M'') of the susceptibilities exhibit maxima at about 14 K, close to the T_c value, and the maximum position is independent of frequency. This confirms the occurrence of ferromagnetic-like LRO. It is noted that the χ_M' peaks at 1, 10, 100, and 1000 Hz are unsymmetrical in shape, with the low temperature sides showing some dependence upon the frequency (it is less appreciable in χ_M'' curves). This indicates the presence of some dynamic relaxation process.

Further information comes from the field-dependent isothermal magnetization measurements (Fig. 3b). For **1**, the initial $M(H)$ curve exhibits the sigmoid shape typical of metamagnetism, which is often observed in layer or chain systems with anisotropy and competing interactions [21]. The slow increase of magnetization in the low field region (0–1.7 kOe) suggests the AF ordering of the spin-canted layers, and the rapid rise in the 1.7–3.3 kOe region indicates that the interlayer AF ordering can be broken up by the applied field generate a WF state in which the spin-canted layers are F-ordered [7e]. The critical field for the AF-to-F transition at 2 K was estimated to be 2.0 kOe, at which the dM/dH curve exhibits a maximum. At 2 K, **1** exhibits hysteresis loops, related to the anisotropy of Ni(II) ion. Compound **1** behaves as a hard magnet with a coercive field of 1.7 kOe and a remnant magnetization of 0.24 N β . $[Ni(4,4'-bipy)(N_3)_2]_n$, (4,4'-bipy = 4,4'-bipyridine), also exhibits a weak ferromagnetism, and shows LRO behaviors combining spin canting and hysteresis loop at low temperature [22]. While $Ni(dca)_2(Mepyz)_2 \cdot H_2O$, (dca = dicyanamide, Mepyz = methylpyrazine), also exhibits a weak ferromagnetism, and LRO behaviors is not observed [23].

In conclusion, we have described the structures and magnetic properties of a new Ni-pyridine-3,5-dicarboxylate-compound **1** that possesses a 3D supramolecular network based on (3,5)-connected helical-armed 2D layers. Interestingly, **1** exhibits a weak ferromagnetism at high temperature (>12.7 K), whereas at low temperature, it shows unusual LRO behaviors combining spin canting (weak antiferromagnetism) and hysteresis loop. The successful synthesis of **1** not only enriches the existing field of pyridine-3,5-dicarboxylate-complexes but also opens possibilities for synthesizing other novel metallic complexes using different appropriate precursors and co-ligands.

Acknowledgment

This work was financially supported by the NSF of China (nos: 21373122, 21301106, 51572152 and 51502155), the NSF of Hubei Province of China (no. 2014CFB277).

Appendix A. Supplementary data

CCDC 1465211 contains the supplementary crystallographic data for **1**. The data can be obtained free of charge via <http://www.ccdc.cam.ac.uk/conts/retrieving.html>, or from the Cambridge Crystallographic Data Centre, 12 Union Road, Cambridges CB2 1EZ, UK; fax: (+44) 1223-336-033; or e-mail: deposit@ccdc.cam.ac.uk. Selected bond lengths and angles for **1**. Additional structural figures, PXRD patterns, TGA curves for complex **1**. Temperature dependent AC susceptibility

components. These data can be found in the supporting file. Supplementary data to this article can be found online at <http://dx.doi.org/10.1016/j.inoche.2016.04.023>.

References

- [1] (a) M.-H. Zeng, Z. Yin, Y.-X. Tan, W.-X. Zhang, Y.-P. He, M. Kurmoo, Nanoporous cobalt(II) MOF exhibiting four magnetic ground states and changes in gas sorption upon post-synthetic modification, *J. Am. Chem. Soc.* 136 (2014) 4680–4688;
- (b) M.-L. Han, Y.-P. Duan, D.-S. Li, H.-B. Wang, J. Zhao, Y.-Y. Wang, Positional isomeric tunable two Co(II) 6-connected 3-D frameworks with pentanuclear to binuclear units: structures, ion-exchange and magnetic properties, *Dalton Trans.* 43 (2014) 15450–15456;
- (c) D.-S. Li, Y.-P. Wu, J. Zhao, J. Zhang, J.Y. Lu, Metal-organic frameworks based upon non-zeotype 4-coordinated topology, *Coord. Chem. Rev.* 261 (2014) 1–27;
- (d) D.-F. Weng, Z.-M. Wang, S. Gao, Framework-structured weak ferromagnets, *Chem. Soc. Rev.* 40 (2011) 3157–3181.
- [2] (a) D.-S. Li, J. Zhao, Y.-P. Wu, B. Liu, L. Bai, K. Zou, M. Du, Co_5/Co_8 -cluster-based coordination polymers showing high-connected self-penetrating networks: syntheses, crystal structures, and magnetic properties, *Inorg. Chem.* 52 (2013) 8091–8098;
- (b) Q. Yue, N.-N. Wang, S.-Y. Guo, L.-L. Liang, E.-Q. Gao, Homochiral and heterochiral Mn(II) coordination frameworks: spontaneous resolution dependent on dipyradyl ligands, *Dalton Trans.* 45 (2016) 1335–1338;
- (c) C. Zhang, M. Zhang, L. Qin, H. Zheng, Crystal structures and spectroscopic properties of metal-organic frameworks based on rigid ligands with flexible functional groups, *Cryst. Growth Des.* 14 (2014) 491–499.
- [3] (a) X.-L. Zhao, W.-Y. Sun, The organic ligands with mixed N-/O-donors used in construction of functional metal-organic frameworks, *CrystEngComm* 16 (2014) 3247–3258;
- (b) H. Li, W. Shi, Z. Niu, J.-M. Zhou, G. Xiong, L.-L. Li, P. Cheng, Remarkable $Ln^{III}_3Fe^{III}_2$ clusters with magnetocaloric effect and slow magnetic relaxation, *Dalton Trans.* 44 (2015) 468–471;
- (c) L.-F. Ma, M.-L. Han, J.-H. Qin, L.-Y. Wang, M. Du, Mn^{II} coordination polymers based on Bi-, Tri-, and tetrานuclear and polymeric chain building units: crystal structures and magnetic properties, *Inorg. Chem.* 51 (2012) 9431–9442.
- [4] (a) T. Gong, X. Yang, Q. Sui, F.-G. Xi, E.-Q. Gao, Magnetic and photochromic properties of a manganese(II) metal-zwitterionic coordination polymer, *Inorg. Chem.* 55 (2016) 96–103;
- (b) D. Sarma, P. Mahata, S. Natarajan, P. Panissod, G. Rogez, M. Drillon, Synthesis, structure, and magnetic properties of a new eight-connected metal-organic framework (MOF) based on Co_4 clusters, *Inorg. Chem.* 51 (2012) 4495–4501;
- (c) H.-S. Lu, L. Bai, W.-W. Xiong, P. Li, J. Ding, G. Zhang, T. Wu, Y. Zhao, J.-M. Lee, Y. Yang, B. Geng, Q. Zhang, Surfactant media to grow new crystalline cobalt 1,3,5-benzenetricarboxylate metal-organic frameworks, *Inorg. Chem.* 53 (2014) 8529–8537.
- [5] (a) L.-C. Gui, X.-J. Wang, Q.-L. Ni, M. Wang, F.-P. Liang, H.-H. Zou, Nanospheric $[M_{20}(OH)_{12}(\text{maleate})_{12}(Me_2NH)_2]^{4+}$ clusters ($M=Co, Ni$) with O_h symmetry, *J. Am. Chem. Soc.* 134 (2012) 852–854;
- (b) E. Freire, M. Quintero, D. VEGA, R. Baggio, Crystal structure and magnetic properties of two new zoledronate complexes: a Mn dimer $[\text{Mn}(\text{II})(\text{H}_3\text{Zol})_2 \cdot (\text{H}_2\text{O})_2]$ and a Fe₁₅ molecular cluster $[\text{Fe}(\text{III})_{15}(\text{Hzol})_{10}(\text{H}_2\text{Zol})_2(\text{H}_2\text{O})_{12}(\text{Cl}_4 \cdot (\text{H}_2\text{O})_2 \cdot \text{Cl}_7 \cdot (\text{H}_2\text{O})_{65}]$ (where $\text{H}_4\text{Zol} = \text{C}_5\text{H}_{10}\text{N}_2\text{O}_2\text{P}_2$ is zoledronic acid), *Inorg. Chim. Acta* 394 (2013) 229–236;
- (c) D.-K. Cao, M.-J. Liu, J. Huang, S.-S. Bao, L.-M. Zheng, Cobalt and manganese diphosphonates with one-, two-, and three-dimensional structures and field-induced magnetic transitions, *Inorg. Chem.* 50 (2011) 2278–2287.
- [6] (a) D. Gatteschi, R. Sessoli, Quantum tunneling of magnetization and related phenomena in molecular materials, *Angew. Chem. Int. Ed.* 42 (2003) 268–297;
- (b) O. Kahn, *Molecular Magnetism*, New York, VCH, 1993.
- [7] (a) O. Sato, J. Tao, Y.-Z. Zhang, Control of magnetic properties through external stimuli, *Angew. Chem. Int. Ed.* 46 (2007) 2152–2187;
- (b) E. Coronado, P. Day, Magnetic molecular conductors, *Chem. Rev.* 104 (2004) 5419–5448;
- (c) D. Maspoch, D. Ruiz-Molina, K. Wurst, N. Domingo, M. Cavallini, F. Biscarini, J. Tejada, C. Rovira, J. Veciana, A nanoporous molecular magnet with reversible solvent-induced mechanical and magnetic properties, *Nat. Mater.* 2 (2003) 190–195;
- (d) E.-Q. Gao, S.-Q. Bai, Z.-M. Wang, C.-H. Yan, Two-dimensional homochiral manganese(II)-azido frameworks incorporating an achiral ligand: partial spontaneous resolution and weak ferromagnetism, *J. Am. Chem. Soc.* 125 (2003) 4984–4985;
- (e) E.-Q. Gao, P.-P. Liu, Y.-Q. Wang, Q. Yue, Q.-L. Wang, Complex long-range magnetic ordering behaviors in anisotropic cobalt(II)-azide multilayer systems, *Chem. Eur. J.* 15 (2009) 1217–1226.
- [8] (a) Q. Chen, M.-H. Zeng, Y.-L. Zhou, H.-H. Zou, M. Kurmoo, Hydrogen-bonded dicubane Co^{II}_8 single-molecule-magnet coordinated by *in situ* solvothermally generated 1,2-bis(8-hydroxyquinolin-2-yl)ethane-1,2-diol arranged in a trefoil, *Chem. Mater.* 22 (2010) 2114–2119;
- (b) L. Qin, Z.-J. Wang, T. Wang, H.-G. Zheng, J.-X. Chen, Coligand-directed synthesis of five Co(II)/Ni(II) coordination polymers with a neutral tetradeятate ligand: syntheses, crystal structures, and properties, *Dalton Trans.* 43 (2014) 12528–12535;

- (c) L.-C. Gui, X.-J. Wang, Q.-L. Ni, M. Wang, F.-P. Liang, H.-H. Zou, Nanospheric $[M_{20}(\text{OH})_{12}(\text{maleate})_{12}(\text{Me}_2\text{NH})_{12}]^{4+}$ clusters ($M=\text{Co, Ni}$) with O_h symmetry, *J. Am. Chem. Soc.* 134 (2012) 852–854;
- (d) M. Kalisz, R.A.A. Cassaro, M.A. Novak, M. Andruh, H.S. Amorim, M.G.F. Vaz, A two-dimensional $\text{Cu}^{\text{II}}\text{-Mn}^{\text{II}}$ heterometallic coordination polymer: structure determination using synchrotron X-ray powder diffraction and magnetic properties, *CrystEngComm* 17 (2015) 7423–7429.
- [9] (a) L. Cañadillas-Delgado, O. Fabelo, J.A. Rodríguez-Velamazán, M.-H. Lemée-Cailleau, S.A. Mason, E. Pardo, F. Lloret, J.-P. Zhao, X.-H. Bu, V. Simonet, C.V. Colin, J. Rodríguez-Carvajal, The role of order-disorder transitions in the quest for molecular multiferroics: structural and magnetic neutron studies of a mixed iron(II)-iron(III) formate framework, *J. Am. Chem. Soc.* 134 (2012) 19772–19781;
- (b) O. Fabelo, L. Cañadillas-Delgado, J. Pasán, F.S. Delgado, F. Lloret, J. Cano, M. Julve, C. Ruiz-Pérez, Study of the influence of the bridge on the magnetic coupling in cobalt(II) complexes, *Inorg. Chem.* 48 (2009) 11342–11351;
- (c) F. Su, L. Lu, S. Feng, M. Zhu, Z. Gao, Y. Dong, Synthesis, structures and magnetic properties in 3d-electron-rich isostructural complexes based on chains with sole *syn-anti* carboxylate bridges, *Dalton Trans.* 44 (2015) 7213–7222;
- (d) G. Rousse, G. Radtke, Y. Klein, H. Ahouri, Long-range antiferromagnetic order in malonate-based on compounds $\text{Na}_2\text{M}(\text{H}_2\text{C}_3\text{O}_4)_2 \cdot 2\text{H}_2\text{O}$ ($\text{M}=\text{Mn, Fe, Co, Ni}$), *Dalton Trans.* (2016), <http://dx.doi.org/10.1039/c5dt04527d>.
- [10] (a) Y.-X. Tan, Y.-P. He, M. Wang, J. Zhang, A water-stable zeolite-like metal-organic framework for selective separation of organic dyes, *RSC Adv.* 4 (2014) 1480–1483;
- (b) F.-C. Liu, Y.-F. Zeng, J.-R. Li, X.-H. Bu, H.-J. Zhang, J. Ribas, Novel 3-D framework nickel(II) complex with azide, nicotinic acid, and nicotinate $^{1-}$ as coligands: hydrothermal synthesis, structure, and magnetic properties, *Inorg. Chem.* 44 (2005) 7298–7300;
- (c) P. Teo, L.L. Koh, T.S.A. Hor, Oligo- and polymeric Pd^{II} and Pt^{II} using pyridyl carboxylate spacers for topology control, *Inorg. Chem.* 47 (2008) 6464–6474.
- [11] (a) W. Chen, H.-M. Yuan, J.-Y. Wang, Z.-Y. Liu, J.-J. Xu, M. Yang, J.-S. Chen, Synthesis, structure, and photoelectronic effects of a uranium-zinc-organic coordination polymer containing infinite metal oxide sheets, *J. Am. Chem. Soc.* 125 (2003) 9266–9267;
- (b) C.-P. Li, J.-M. Wu, M. Du, Exceptional crystallization diversity and solid-state conversions of Cd^{II} coordination frameworks with 5-bromonicotinate directed by solvent media, *Chem. Eur. J.* 18 (2012) 12437–12445;
- (c) Q. Yang, J.-P. Zhao, W.-C. Song, X.-H. Bu, Two azido-bridged cobalt(II) coordination polymers with nicotinate co-ligand: synthesis, structures and magnetic properties, *Dalton Trans.* 41 (2012) 6272–6276.
- [12] (a) J.-J. Hou, R. Zhang, Y.-L. Qin, X.-M. Zhang, From (3,6)-connected kgd, chiral anh to (3,8)-connected tfz-d nets in low nuclear metal cluster-based networks with triangular pyridinedicarboxylate ligand, *Cryst. Growth Des.* 13 (2013) 1618–1625;
- (b) T.K. Maji, G. Mostafa, R. Matsuda, S. Kitagawa, Guest-induced asymmetry in metal-organic porous solid with reversible single-crystal-to-single-crystal structural transformation, *J. Am. Chem. Soc.* 127 (2005) 17152–17153;
- (c) L.-L. Wen, D.-B. Dang, C.-Y. Duan, Y.-Z. Li, Z.-F. Tian, Q.-J. Meng, 1D helix, 2D brick-wall and herringbone, and 3D interpenetration d^{10} metal-organic framework structures assembled from pyridine-2,6-dicarboxylic acid N-oxide, *Inorg. Chem.* 44 (2005) 7161–7170.
- [13] (a) A. Calderon-Casado, G. Barandika, B. Bazan, M.-I. Urtiaga, M.-I. Arriortua, Unprecedented coordination modes for PDC (pyridine-2,5-dicarboxylate) in polymorphic 3D heterobimetallic compounds α - and β -[$\text{MNa}_2(\text{PDC})_2(\text{H}_2\text{O})_4$], with $\text{M}=\text{Ni, Co}$, *CrystEngComm* 12 (2010) 1784–1789;
- (b) X.-L. Li, G.-Z. Liu, L.-Y. Xin, L.-Y. Wang, A novel metal-organic framework displaying reversibly shrinking and expanding pore modulation, *CrystEngComm* 14 (2012) 5757–5760;
- (c) Y. Lv, Y. Qi, L. Sun, F. Luo, Y. Che, J. Zheng, Construction of metal-organic frameworks with the pyridine-3,5-dicarboxylate anion and bis(imidazole) ligands: synthesis, structure, and thermostability studies, *Eur. J. Inorg. Chem.* (2010) 5592–5596.
- [14] (a) A. Cheansirisomboon, C. Pakawatchai, S. Yongme, 2D-1D structural phase transformation of Co^{II} 3,5-pyridicarboxylate frameworks with chromatotropism, *Dalton Trans.* 41 (2012) 10698–10706;
- (b) Y.-G. Huang, X.-T. Wang, F.-L. Jiang, S. Gao, M.-Y. Wu, Q. Gao, W. Wei, M.-C. Hong, Cobalt-lanthanide coordination polymers constructed with metalloligands: a ferromagnetic coupled quasi-1D Dy^{3+} chain showing slow relaxation, *Chem. Eur. J.* 14 (2008) 10340–10347.
- [15] (a) M. Du, C.-P. Li, C.-S. Liu, S.-M. Fang, Design and construction of coordination polymers with mixed-ligand synthetic strategy, *Coord. Chem. Rev.* 257 (2013) 1282–1305;
- (b) M.-L. Han, Y.-P. Duan, D.-S. Li, G.-W. Xu, Y.-P. Wu, J. Zhao, A series of divalent metal coordination polymers based on isomeric tetracarboxylic acids: synthesis, structures and magnetic properties, *Dalton Trans.* 43 (2014) 17519–17527;
- (c) L. Ma, X. Wang, D. Deng, F. Luo, B. Ji, J. Zhang, Five porous zinc(II) coordination polymers functionalized with amide groups: cooperative and size-selective catalysis, *J. Mater. Chem. A* 3 (2015) 20210–20217.
- [16] (a) M.-L. Han, X.-H. Chang, X. Feng, L.-F. Ma, L.-Y. Wang, Temperature and pH driven self-assemble of Zn^{II} coordination polymers: crystal structures, supramolecular isomerism, and photoluminescence, *CrystEngComm* 16 (2014) 1687–1695;
- (b) J. Wang, X. Zhu, Y.-F. Cui, B.-L. Li, H.-Y. Li, A polythreading coordination array formed from 2D grid networks and 1D chains, *CrystEngComm* 13 (2011) 3342–3344;
- (c) J. Zhao, W.-W. Dong, Y.-P. Wu, Y.-N. Wang, C. Wang, D.-S. Li, Q.-C. Zhang, Two (3,6)-connected porous metal-organic frameworks based on linear trinuclear $[\text{Co}_3(\text{COO})_6]$ and paddlewheel dinuclear $[\text{Cu}_2(\text{COO})_4]$ SBUs: gas adsorption, photocatalytic behaviour, and magnetic properties, *J. Mater. Chem. A* 3 (2015) 6962–6969.
- [17] (a) Z.-X. Xu, Y.-L. Ma, Y. Xiao, L. Zhang, J. Zhang, A series of homochiral helical metal-organic frameworks based on proline derivatives, *Cryst. Growth Des.* 15 (2015) 5901–5909;
- (b) M.-L. Han, L. Bai, P. Tang, X.-Q. Wu, J. Zhao, D.-S. Li, Y.-Y. Wang, Biphenyl-2,4,6,3',5'-pentacarboxylic acid as a tecton for six new Co^{II} coordination polymers: pH and N-donor ligand-dependent assemblies, structure diversities and magnetic properties, *Dalton Trans.* 44 (2015) 14673–14686;
- (c) L. Bai, H.-B. Wang, D.-S. Li, Y.-P. Wu, J. Zhao, L.-F. Ma, A new penta-carboxylate and N-donor ligand co-regulate 3D Co^{II} -MOF with tcj/hc topology: synthesis, structure and magnetic property, *Inorg. Chem. Commun.* 44 (2014) 188–190;
- (d) J. Zhao, D.-S. Li, X.-J. Ke, B. Liu, K. Zou, H.-M. Hu, Auxiliary ligand-directed structural variation from 2D → 3D polythreaded net to 3-fold interpenetrating 3D pillar-layered framework: syntheses, crystal structures and magnetic properties, *Dalton Trans.* 41 (2012) 2560–2563.
- [18] (a) Z.-Q. Yu, M. Pan, J.-J. Jiang, Z.-M. Liu, C.-Y. Su, Anion modulated structural diversification in the assembly of Cd^{II} complexes based on a balance-like dipodal ligand, *Cryst. Growth Des.* 12 (2012) 2389–2396;
- (b) M. Pan, C.-Y. Su, Coordination assembly of Borromean structures, *CrystEngComm* 16 (2014) 7847–7859;
- (c) C. Yan, Y.-Z. Fan, L. Chen, M. Pan, L.-Y. Zhang, J.-J. Jiang, C.-Y. Su, Time controlled structural/packing transformation and tunable luminescence of Cd^{II} -chloride-triBZ-ntb coordination assemblies: an experimental and theoretical exploration, *CrystEngComm* 17 (2015) 546–552.
- [19] Preparation of $[\text{Ni}(\text{pdc})(\text{bib})] \cdot 2\text{H}_2\text{O}$ (**1**). A mixture of H_2pdc (0.10 mmol, 16.1 mg), bib (0.10 mmol, 19.0 mg), $\text{Ni}(\text{OAc})_2 \cdot 4\text{H}_2\text{O}$ (0.10 mmol, 24.9 mg), and H_2O (8 mL) was placed in a 25 mL Teflon-lined stainless steel vessel, heated to 140 °C for 120 h, then the reaction system was cooled to room temperature and green block crystals were obtained. Yield: 29.2 mg, 65% (based on Ni^{II}). Elemental analysis (%): calcd for $(\text{C}_{17}\text{H}_{21}\text{Ni}_5\text{O}_6)$: C, 45.37; H, 4.70; N, 15.56; Found: C, 45.30; H, 4.62; N, 15.51. IR (KBr, cm^{-1}): 3450 w, 1637 s, 1580 m, 1522 m, 1390 s, 780 m, 762 s, 665 m.
- [20] The crystallographic data for **1** were carried out on a Bruker SMART APEX CCD diffractometer with graphite-monochromated Mo K α radiation ($\lambda = 0.71073 \text{ \AA}$) at room temperature using the ϕ/ω scanning technique. The structures were solved using direct methods and successive Fourier difference synthesis (SHELXS-97) [24], and refined using the full-matrix least-squares method on F^2 with anisotropic thermal parameters for all non-hydrogen atoms (SHELXL-97) [24]. An empirical absorption correction was applied using the SADABS program. The hydrogen atoms were placed in calculated positions. Selected bond lengths and angles are summarized in Table S1. Crystal data for **1**: $\text{C}_{17}\text{H}_{21}\text{Ni}_5\text{O}_6$ ($M_r = 450.10$), monoclinic, $P2_1/n$, $a = 9.4244(7)$, $b = 12.4821(10)$, $c = 16.2475(13) \text{ \AA}$, $\beta = 96.7390(10)^\circ$, $V = 1898.1(3) \text{ \AA}^3$, $Z = 4$, $\rho = 1.575 \text{ g cm}^{-3}$, $S = 0.951$, and $R = 0.0476$, $wR = 0.0637$ ($I > 2\sigma(I)$), $R = 0.0686$, $wR = 0.0685$ (all data).
- [21] R.L. Carlin, *Magnetochemistry*, Springer-Verlag, Heidelberg, 1986.
- [22] S. Martin, M.G. Barandika, L. Lezama, J. Luis Pizarro, Z.E. Serna, J.I.R. De Larramendi, M.I. Arriortua, T. Rojo, R. Cortés, Weak M^{II} -azide-4,4'-bipy ferromagnets based on unusual diamondoid ($\text{M}=\text{Mn}$) and 2D arrays ($\text{M}=\text{Co, Ni}$), *Inorg. Chem.* 40 (2001) 4109–4115.
- [23] A.M. Kutasi, A.R. Harris, S.R. Batten, B. Moubaraki, K.S. Murray, Coordination polymers of dicyanamide and methylpyrazine: syntheses, structures, and magnetic properties, *Cryst. Growth Des.* 4 (2004) 605–610.
- [24] G.M. Sheldrick, A short history of SHELX, *Acta Crystallogr. A* 64 (2008) 112–122.